

Mechanism of quantum effects in hydrogen-bonded crystals of the $K_3H(SO_4)_2$ group

Dalibor Merunka and Boris Rakvin*

Ruđer Bošković Institute, Bijenička cesta 54, P.O. BOX 180, 10002 Zagreb, Croatia

(Received 2 February 2009; revised manuscript received 31 March 2009; published 24 April 2009)

The complete isotope effect and quantum paraelectricity in hydrogen-bonded crystals of the $K_3H(SO_4)_2$ group are usually attributed to the proton tunneling and geometric isotope effect. However, a mechanism of the quantum effects is not unambiguously determined because neutron-scattering experiments indicate different forms of hydrogen-bond proton potential. The quantum effects and contradictory experimental results are accounted for by the model where the proton potential is strongly affected by a low-frequency heavy-atom mode.

DOI: [10.1103/PhysRevB.79.132108](https://doi.org/10.1103/PhysRevB.79.132108)

PACS number(s): 77.84.Fa, 77.80.Bh

The H-bonded crystals of $K_3H(SO_4)_2$ (KHS) group are of great technological and theoretic interest because they exhibit the superprotonic conductivity at high temperatures¹ and the intriguing quantum effects at low temperatures.^{2,3} Several KHS crystals show a complete H/D isotope effect, which means that they undergo a low-temperature antiferroelectric phase transition in the deuterated, but not in protonated form. Also, the absence of phase transition is usually ascribed to the quantum paraelectric state of protonated crystals, in which quantum fluctuations of atoms suppress the phase transition. Similar effects were observed in the more widely investigated material $SrTiO_3$, which is a quantum paraelectric in its natural form and a ferroelectric in the ¹⁸O-enriched form.^{4,5} However, while the ferroelectricity induced by ¹⁶O/¹⁸O substitution in $SrTiO_3$ is simply attributed to the suppression of zero-point energy by the mass increase of O atoms,⁶ the mechanism of quantum effects in KHS crystals is not so straightforward. To elucidate this mechanism, as well as the mechanism of proton conductivity, the essential step is to determine the proton potential in H bond. However, the neutron-scattering experiments, which are the best methods for providing this information, give controversial results.^{2,7,8} The strong low-energy peaks observed in the inelastic neutron-scattering spectra of KHS and $Rb_3H(SO_4)_2$ (RHS) were ascribed to the proton-tunneling splitting in double-well H-bond potential,⁷ which supports the proton-tunneling mechanism of quantum effects.³ Also, the neutron-diffraction data for $K_3H(SeO_4)_2$ (KHSe) imply that the proton is disordered over two positions along the H bond above the critical temperature T_c , which indicates a double-well proton potential.⁸ However, the double-well potential that reproduces the inelastic neutron-scattering spectra of RHS is

too wide to reproduce the proton momentum distribution in RHS measured by the neutron Compton scattering, which corresponds to the ground-state momentum distribution of proton in a single-well potential.² On the other hand, the double Morse potential that approximates well this single-well potential shows some inconsistencies with experimental data.² It is so narrow that we can hardly explain the fact that the proton position distribution in KHSe is two-peaked. Additionally, the proton excitation energies in this potential (~ 100 meV) are much higher than the energies of strong peaks in inelastic neutron-scattering spectra (~ 5 meV). Finally, this potential implies that the H-bond length R (O-O distance) has the value 2.4 Å in RHS, while the diffraction data⁸⁻¹¹ imply quite longer H bonds in KHS crystals (see Table I). In the present Brief Report, we provide an explanation of the quantum effects and contradictory results in KHS crystals by employing a simple model, which uses the idea¹² that the H-bond potential in a local dimer is strongly affected by a vibrational mode of heavy atoms.

In the concept of quantum temperature, the effect of quantum fluctuations are taken into account by replacement of the temperature T by a quantum temperature $T_Q = T_s \coth(T_s/T)$ with the saturation temperature T_s .¹³ Thus, a ferroelectric system susceptibility follows the Barrett law⁴ rather than the classical Curie-Weiss law and T_c decreases from a classical critical temperature T_0 to $T_s / \tanh^{-1}(T_s/T_0)$. The small effect of quantum fluctuations in a classical ferroelectric regime $T_s < T_0/2$ becomes significant in a quantum ferroelectric regime $T_0/2 < T_s < T_0$; finally, the phase transition is suppressed in the quantum paraelectric regime $T_s > T_0$. Since the susceptibility of many quantum paraelectrics follows the Barrett law, the concept of quantum temperature has a strong

TABLE I. Experimental values in protonated (H) and deuterated (D) KHS crystals for the critical temperature T_c , the temperature T_1 corresponding to excitation energy in calorimetric measurements and inelastic neutron-scattering spectra (in parentheses), and the hydrogen-bond length R near T_c (or 0 K if the phase transition is absent).

Crystal	T_{cH} (K)	T_{cD} (K)	T_{1H} (K)	R_H (Å)	R_D (Å)
KHSe	21	105	52(–)	2.495	2.533
RHSe	no	92	53 (58)	2.473	2.518
KHS	no	84	–(82)	2.468	2.498
RHS	no	71	62 (63)	2.465	2.505

experimental support.^{4–6,13–15} The theoretical considerations show that T_0 mainly depends on (anti)ferroelectric interaction between elementary dipoles and that $T_1=2T_s$ corresponds to an excitation energy of the dipole.^{13,14} In the order-disorder (anti)ferroelectrics, the dipole is subjected to a local double-well potential and $T_1=\Delta/k$, where Δ is the quantum-tunneling energy splitting. In the displacive (anti)ferroelectrics, the dipole is an anharmonic oscillator and $T_1=\hbar\Omega_0/k$, where Ω_0 is renormalized frequency. The mass change of atoms upon isotope substitution generally affects the excitation energy of elementary dipole more than the interaction energy between the dipoles, so that T_s is expected to be more sensitive than T_0 to isotope exchange. This expectation is confirmed in the ¹⁸O-enriched SrTiO₃, where T_s decreases with increasing ¹⁸O exchange rate, while T_0 remains constant.⁶ Similarly, the H/D isotope effect in H-bonded (anti)ferroelectrics was ascribed to the isotope-dependent T_s that corresponds to the tunneling energy of proton (deuteron) in a double-well H-bond potential.³ Both the tunneling energy and T_s increase upon D/H replacement due to the mass decrease, which explains why the phase transition has lower T_c or is absent in the protonated crystal. However, recent experimental results for ferroelectric KH₂PO₄ (KDP), whose T_c strongly increases upon H/D substitution, contradict this mechanism.^{14,16} They indicate a low value of T_s compared with the proton-tunneling energy Δ/k and T_c , which suggests that T_s does not correspond to the proton-tunneling energy and does not cause the isotope effect. These unexpected results have been explained by a simple model where the tunneling protons in H bonds interact with the dipoles produced on neighboring PO₄ groups,¹⁷ using the idea that the excitation energy of dipole is much lower than Δ , so that the protons adiabatically follow changes of the dipoles.¹⁸ Here, a similar mechanism is applied for the KHS crystals.

The KHS crystals contain a 0D network of H bonds, which link two SO₄(SeO₄) tetrahedra into isolated dimers.¹⁹ The room-temperature symmetry is the same for all crystals, except for Cs₃H(SeO₄)₂ which is not considered here. The deuterated crystals undergo antiferroelectric phase transition at 71–105 K, and a large effect of D/H replacement is manifested by both the small value of T_c in KHSe and the absence of phase transition in RHSe, KHS, and RHS (Table I).^{8,19} The calorimetric measurements indicate a classical order-disorder type of phase transition in the deuterated crystals and an excess heat capacity at low temperatures in the protonated crystals.^{3,20–22} The excess heat capacity was attributed to the excitation energy kT_1 responsible for the quantum paraelectricity and the estimated values^{20–22} of T_1 correspond well with the positions of strong low-energy peaks in inelastic neutron-scattering spectra^{7,12} (Table I). The energy kT_1 is ascribed to the proton-tunneling energy Δ in the proton-tunneling mechanism of complete isotope effect, where a high value of Δ in protonated crystal causes the quantum paraelectric state $T_1>2T_0$, while a reduced value of Δ in deuterated crystal causes the classical order-disorder phase transition $T_1<T_0\approx T_c$.^{3,20} However, the neutron Compton scattering data indicate a single-well H-bond potential in RHS,² which supports an alternative mechanism where a single-well H-bond potential in protonated crystal prevents the phase transition, while a double-well potential in deuter-

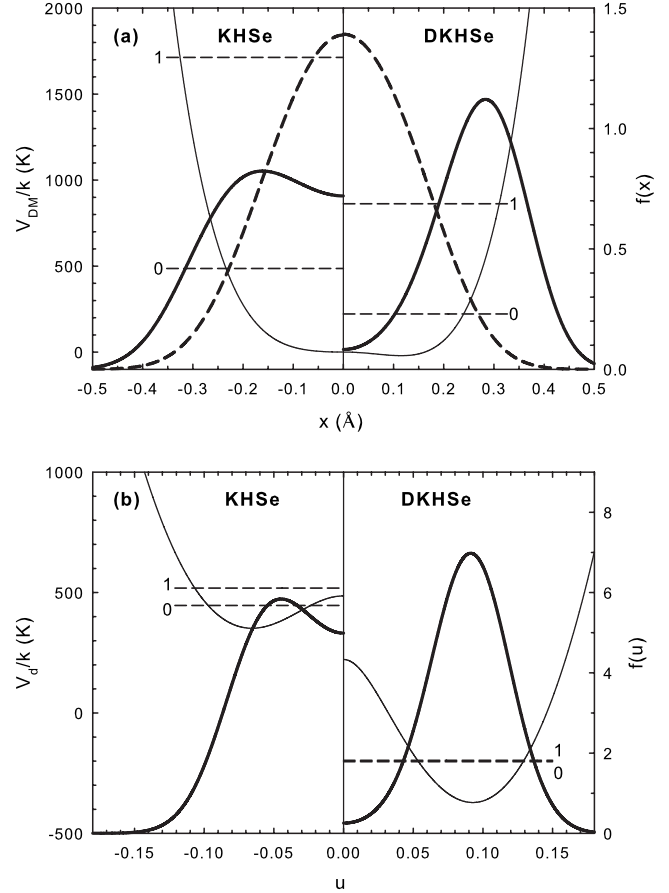


FIG. 1. (a) The energy levels of proton and deuteron (dashed lines) and their ground-state distributions $f_0(x)$ (thick dashed lines) in the double Morse potentials $V_{DM}(x)$ (full lines) of KHSe and DKHSe. The distributions $f(x)$ of proton and deuteron at T_c in the dipole model are shown by thick full lines. (b) The energy levels of dipole (dashed lines) and its distributions at $T_c f(u)$ (thick full lines) in the potentials $V_d(u)$ (full lines) of KHSe and DKHSe in the dipole model.

ated crystal, resulting from the increase in R (geometric isotope effect), promotes the phase transition.⁹ The double Morse potential that approximates well the H-bond potential from neutron Compton scattering study has the parameters $D/k=3.39\times 10^4$ K, $a=1.96$ Å⁻¹, and $r_0=0.9$ Å,² which are used here to construct a simple proton model for KHS crystals. In this model, the proton moving along the H bond has the Hamiltonian $H_p=p^2/2m+V_{DM}(x)$, where m is the proton mass, x is its displacement from the H-bond center, p is its momentum, and the double Morse potential is

$$V_{DM}(x)=2D(e^{-2z}\cosh 2ax-2e^{-z}\cosh ax) \quad (1)$$

with $z=a(R/2-r_0)$. To apply the model for KHSe and K₃D(SeO₄)₂ (DKHSe), the experimental values of R are used (Table I) and the energies E_i and wave functions $\Psi_i(x)$ of H_p are calculated. The calculated excitation energies $\Delta_x/k=(E_1-E_0)/k$ of the proton in KHSe (1230 K) and the deuteron in DKHSe (640 K) [Fig. 1(a)] are much higher than the measured T_1 (Table I). Also, their ground-state position distributions $f_0(x)=|\Psi_0(x)|^2$ are single-peaked [Fig. 1(a)], while

the experimental distributions near above T_c show two peaks separated by $\delta=0.32$ Å in KHSe and $\delta=0.55$ Å in DKHSe.⁸ Because other protonated and deuterated KHS crystals have shorter H bonds than KHSe and DKHSe, respectively, they have higher Δ_x and narrower $f_0(x)$, which implies that the model cannot explain properties of the KHS crystals.

To improve the model, a coupling between the proton and a dipole moment μ produced by a vibrational mode of dimer is introduced.¹² In the simplest case, the dipole is harmonic oscillator coupled through the bilinear term $-K\mu x$ to the proton displacement, where K is the dipole-proton coupling constant. Defining the dimensionless variable proportional to the dipole moment $u=K\mu/2Da$, where D and a are the parameters of $V_{DM}(x)$ from Eq. (1), the dimer Hamiltonian can be put in the form

$$H = P^2/2M + p^2/2m + M\omega_0^2 u^2/2 - 2Daux + V_{DM}(x). \quad (2)$$

Here, P is the momentum corresponding to u , $M\omega_0^2$ is the elastic constant, and $\hbar\omega_0$ is the bare excitation energy of dipole. As in the case of KDP, it is assumed that $\hbar\omega_0 < \Delta_x$ holds and that the proton adiabatically follows the dipole.^{17,18,23} In this approximation, the dipole Hamiltonian at temperatures of interest ($kT \ll \Delta_x$) is

$$H_d = P^2/2M + V_d(u), \quad (3)$$

where $V_d(u) = M\omega_0^2 u^2/2 + E_0(u)$ is the effective dipole potential and $E_0(u)$ is the ground-adiabatic-state energy of proton obtained from the equation

$$(H_p - 2Daux)\Psi_0(x;u) = E_0(u)\Psi_0(x;u). \quad (4)$$

Now, a simple dipole model is constructed, where a dipole-dipole interaction between the dimers produces antiferroelectric phase transition, so that the effective single-dipole Hamiltonian in the mean-field approximation is $H_c = H_d - J\langle u \rangle u$, where J is the effective dipole-dipole interaction constant. The dipole model is applied for KHSe and DKHSe by calculating $E_0(u)$ and the wave functions $\Psi_0(x;u)$ from Eq. (4) for the experimental values of R (Table I). To obtain T_c and the proton distribution $f(x) = f(u)|\Psi_0(x;u)|^2$ at T_c for various values of the parameters $M\omega_0^2$, $\hbar\omega_0$, and J in the mean-field approximation,²⁴ the energies ε_i and wave functions $\Phi_i(u)$ of H_d Eq. (3) are calculated, together with the dipole distribution at T_c given by $f(u) = \sum_i p_i |\Phi_i(u)|^2$, where $p_i = e^{-\varepsilon_i/kT_c} / \sum_j e^{-\varepsilon_j/kT_c}$. For the obtained results to reproduce $T_c = 105$ K and $\delta = 0.55$ Å in DKHSe and $T_c = 21$ K in KHSe,⁸ the model parameters are uniquely determined to be $M\omega_0^2/k = 3.94 \times 10^5$ K, $\hbar\omega_0/k = 446$ K, and $J/k = 1.24 \times 10^4$ K. The parameter $\hbar\omega_0/k$ is lower than Δ_x/k of proton in KHSe (1230 K) and deuteron in DKHSe (640 K), which justifies the applied adiabatic approximation. The results show that $V_d(u)$ has two wells and that $f(u)$ has two peaks in both crystals [Fig. 1(b)]. The excitation energy $\Delta_u = \varepsilon_1 - \varepsilon_0$ corresponds to the dipole-tunneling energy. Its value in KHSe $\Delta_u/k = 72$ K is close to the estimated T_1 (Table I) and its small value in DKHSe $\Delta_u/k = 6$ K supports the classical order-disorder phase transition. The calculated $f(x)$ also have two peaks [Fig. 1(a)]. They are separated by $\delta = 0.55$ Å in DKHSe, as required, and by $\delta = 0.33$ Å in KHSe, which is close to the experimental value $\delta = 0.32$ Å.⁸

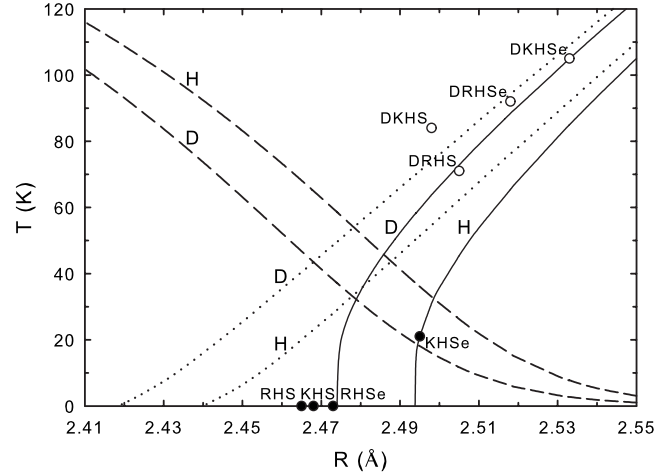


FIG. 2. The dependencies of the critical temperature T_c (full line), the critical temperature for classical dipoles T_0 (dotted line), and the temperature corresponding to the half of dipole-excitation energy $\Delta_u/2k$ (dashed line) on the hydrogen-bond length R of the protonated (h) and deuterated (d) systems in the dipole model. The full and open circles represent the experimental R and T_c from Table I for protonated and deuterated crystals, respectively, where $T_c = 0$ K is taken if the phase transition is absent.

The model is applied to other KHS crystals by keeping constant the adjusted parameters and calculating T_c , $\Delta_u/2k$, and T_0 (the critical temperature for classical dipoles in the mean-field approximation) as a function of R (Fig. 2). The T_c - R and T_0 - R dependencies predict the absence of phase transition and the quantum paraelectric regime ($T_0 > 0$ K) in the protonated crystals. Also, they reproduce well the measured T_c in the deuterated crystals and their classical regime $T_0 \approx T_c$. The order-disorder regime is also reproduced because the calculated potentials $V_d(u)$ keep a double-well form. The dipole-excitation energy Δ_u , which controls the degree of quantum behavior, has sufficiently high values in protonated crystals ($\Delta_u/2k > T_0$) to produce the quantum paraelectric state and sufficiently low values in deuterated ones ($\Delta_u/k < T_0$) for the classical phase transitions (Fig. 2). Its value in protonated crystals $\Delta_u/k \approx 130$ K is about twice higher than the experimental T_1 (Table I). The complete isotope effect is combined effect of the higher Δ_u and the lower T_0 in protonated systems (Fig. 2), which is caused by the mass effect (H having the lower mass than D) and the geometric effect (the lower R in protonated crystal) on the ground-adiabatic-state energy. This mechanism contrasts with the proton-tunneling mechanism, where the proton-tunneling energy Δ_x controls quantum behavior and the increase in Δ_x upon D/H replacement causes the complete isotope effect.³ The geometric effect contributes more than the mass effect to the changes in Δ_u and T_0 between the protonated and deuterated systems, which is consistent with the alternative mechanism of complete isotope effect.⁹ However, this mechanism assumes that the phase transition is absent in KHS because the H-bond potential has a single well below the critical H-bond length $r_c = 2.473$ Å, where the transformation from the double- to the single-peaked proton position distribution was observed.⁹ Here, $f(x)$ for protonated crystal at $T = 0$ K transforms at nearly same $r_c = 2.476$ Å, while the

H-bond potential $V_{\text{DM}}(x)$ transforms from the single- to the double-well potential at much higher $R=2.51 \text{ \AA}$,² which is the result of strong dipole-proton coupling. Finally, a strong effect of the dipole mode on the proton momentum distribution $n(p)$ can explain why $R=2.4 \text{ \AA}$ from the neutron Compton scattering study on RHS (Ref. 2) is lower than $R=2.465 \text{ \AA}$ estimated from diffraction experiments.¹¹ To illustrate this, the ground-state momentum distribution of proton in the potential $V_{\text{DM}}(x)$ with $R=2.4 \text{ \AA}$ was calculated, corresponding to the measured $n(p)$ in neutron Compton scattering study. It was found that $\sigma=4.18 \text{ \AA}^{-1}$, where $\sigma^2=\langle p^2 \rangle$. On the other hand, $n(p)$ in the model is given by the ground-state momentum distribution $n(p,u)$ of proton in the potential $V_{\text{DM}}(x)-2D_{\text{aux}}$ integrated over $f(u)$. This distribution has the same σ value for higher $R=2.43 \text{ \AA}$ and only slightly lower value $\sigma=4.13 \text{ \AA}^{-1}$ for $R=2.465 \text{ \AA}$. This indicates that the underestimated R in neutron Compton scattering study is the result of neglected dipole-proton coupling.

In summary, the assumed double-well H-bond potential in KHS crystals^{3,7} cannot explain the wide proton momentum distribution from the neutron Compton scattering study on RHS,² while the potential from this study cannot explain the

two-peaked proton position distributions⁸ and the low excitation energies that control quantum behavior of the crystals.^{7,12,20-22} This inconsistency indicates that the proton does not reside in a well-defined single-particle potential, but rather in a potential that is strongly affected by a local vibrational mode.¹² In the presented model, the proton residing in the potential obtained from neutron Compton scattering study couples strongly to the dipole produced by a low-frequency mode of dimer and the dimers interact with the dipole-dipole interaction. This leads to the mechanism of quantum effects similar to that in KDP.^{17,18,23} The measured low-energy excitations correspond to those of dipole in the effective potential determined by the ground-adiabatic-state energy of proton. The isotope effect is caused by different effective potentials in protonated and deuterated crystals due to the mass effect and the geometric effect. Also, the model reproduces the measured proton position and momentum distributions for the experimental H-bond lengths.

This work was supported by the Croatian Ministry of Science, Education and Sports under Grant No. 098-0982915-2939.

*Corresponding author; FAX: +3851-4680-245; rakvin@irb.hr

¹A. R. Lim, J. Appl. Phys. **104**, 124107 (2008); S. M. Haile, D. A. Boysen, C. R. I. Chisholm, and R. B. Merle, Nature (London) **410**, 910 (2001).

²D. Homouz, G. Reiter, J. Eckert, J. Mayers, and R. Blinc, Phys. Rev. Lett. **98**, 115502 (2007).

³Y. Moritomo, Y. Tokura, N. Nagaosa, T. Suzuki, and K. Kumagai, Phys. Rev. Lett. **71**, 2833 (1993).

⁴J. H. Barrett, Phys. Rev. **86**, 118 (1952).

⁵M. Itoh, R. Wang, Y. Inaguma, T. Yamaguchi, Y.-J. Shan, and T. Nakamura, Phys. Rev. Lett. **82**, 3540 (1999).

⁶R. Wang and M. Itoh, Phys. Rev. B **64**, 174104 (2001).

⁷F. Fillaux, A. Lautie, J. Tomkinson, and G. J. Kearly, Chem. Phys. **154**, 135 (1991).

⁸N. Onoda-Yamamuro, O. Yamamuro, T. Matsuo, M. Ichikawa, R. M. Ibberson, and W. I. F. David, J. Phys.: Condens. Matter **12**, 8559 (2000).

⁹Y. Noda, H. Kasatani, Y. Watanabe, and H. Terauchi, J. Phys. Soc. Jpn. **61**, 905 (1992); Y. Noda, J. Korean Phys. Soc. **27**, S156 (1994).

¹⁰M. Ichikawa, T. Gustafsson, and I. Olovsson, Acta Crystallogr. C **48**, 603 (1992); R. Melzer, R. Sonntag, and K. S. Knight, *ibid.* **52**, 1061 (1996).

¹¹S. P. Dolin, A. A. Levin, T. Yu. Mikhailova, M. V. Solin, N. S. Strokach, and N. I. Kirillova, Int. J. Quantum Chem. **96**, 247

(2004).

¹²S. Ikeda and Y. Yamada, Physica B **213-214**, 652 (1995).

¹³S. A. Prosandeev, W. Kleemann, B. Westwanski, and J. Dec, Phys. Rev. B **60**, 14489 (1999).

¹⁴S. Endo, K. Deguchi, and M. Tokunaga, Phys. Rev. Lett. **88**, 035503 (2002).

¹⁵S. Horiuchi, Y. Okimoto, R. Kumai, and Y. Tokura, Science **299**, 229 (2003).

¹⁶G. F. Reiter, J. Mayers, and P. Platzman, Phys. Rev. Lett. **89**, 135505 (2002).

¹⁷D. Merunka and B. Rakvin, Phys. Rev. B **76**, 140101(R) (2007); Ferroelectrics **370**, 176 (2008).

¹⁸H. Sugimoto and S. Ikeda, Phys. Rev. Lett. **67**, 1306 (1991).

¹⁹K. Gesi, J. Phys. Soc. Jpn. **61**, 162 (1992).

²⁰T. Matsuo, K. Kohno, and M. Ichikawa, J. Korean Phys. Soc. **29**, S432 (1996); K. Kohno, T. Matsuo, and M. Ichikawa, *ibid.* **32**, S393 (1998).

²¹M. Ichikawa and T. Matsuo, J. Mol. Struct. **378**, 17 (1996).

²²T. Matsuo, N. Tanaka, M. Fukai, O. Yamamuro, A. Inaba, and M. Ichikawa, Thermochim. Acta **403**, 137 (2003); T. Matsuo, J. Korean Phys. Soc. **29**, S409 (1996).

²³D. Merunka and B. Rakvin, Struct. Bonding (Berlin) **124**, 149 (2007).

²⁴V. V. Savkin, A. N. Rubtsov, and T. Janssen, Phys. Rev. B **65**, 214103 (2002).